

Comparative Study of Corrosion Inhibition Effect for Ordinary Steel in HCl 5.0 M

O. Fergachi^{a,*}, M. Rbaa^b, M. Ouakki^c, R. Touir^{a,d}, F. Benhiba^e, B. Lakhrissi^b, H. Oudda^e,

M. Ebn Touhami^a

^aIbn Tofail University, Faculty of Science, Laboratory of Advanced Materials and Process Engineering, PB 133, Kenitra, Morocco.

^bIbn Tofail University, Faculty of Sciences, Department of Chemistry, Laboratory Agro-Resources, Polymers and Process Engineering, PO Box 133, 14000 Kenitra, Morocco.

^cIbn Tofail University, Faculty of Science, Laboratory of Materials, Electrochemistry and Environment, PB 133, 14000 Kenitra, Morocco.

^dRegional Center for Education and Training, 14000 Kenitra, Morocco.

^eIbn Tofail University, Faculty of Science, Laboratory of Separation Processes, 14000 Kenitra, Morocco.

Received: October 19, 2021; Revised: March 10, 2022; Accepted: March 31, 2022

In the present work the influence of the two organic inhibitors, namely : phenyl (2- (3,4,5 trimethoxyphenyl) -1H-benzo [d] imidazol-1-yl) methanone (P3) and (2- (4 -methoxyphenyl) -1H-benzo [d] imidazol-1-yl) (phenyl) methanone (P4) on the ordinary steel corrosion in 5.0 M HCl solution was investigated by using electrochemical measurements, scanning electron spectroscopy (SEM) coupled with Energy Dispersive Spectroscopy (EDX), UV-visible spectroscopy and theoretical study. The obtained results showed that these compounds act as mixed inhibitors. It is obtained that the inhibition efficiency increases with their concentrations and reaches 97.0% and 91.3% at 10^{-3} M of P3 and P4, respectively. These findings were confirmed by the electrochemical impedance spectroscopy measurements, where the transfer resistance values increase with the concentrations. In addition, the effect of temperature range from 298 K to 328 K was investigated and indicated that P3 and P4 keep their performance at height temperature. Moreover, density functional theory explained the relationship between the molecular structure of imidazole derivatives and inhibition performance obtained experimentally. Additionally, the morphological surface and EDX analyses indicated that these compounds act by the formation of a protective layer on the ordinary steel surface. In order to confirm the possibility of the formation of P3-Fe and P4-Fe complexes, the UV-Visible absorption spectra was used. The obtained results indicated the formation of a complex between Fe^{2+} and molecules inhibitors.

Keywords: Imidazole derivatives, Ordinary steel, Corrosion inhibition, 5 M HCl, DFT calculations, SEM/EDX analyse, UV-visible spectroscopy.

1. Introduction

The importance of protection of iron materials against corrosion in acidic solutions has been increased by the fact that they are more susceptible to be attacked in aggressive industrial environments. Thus, the corrosion is a major industrial problem (estimated at 3.4% of world gross product in 2013), which cover all the means of combating corrosion, the replacement of corroded parts or structures and the direct and indirect consequences of accidents due to corrosion¹. In addition, hydrochloric acid, for example, was often used as a pickling acid for iron and its alloys to remove undesirable corrosion products². This acid will cause metal corrosion upon the already cleaned surface after the corrosion products elimination. So, in order to reduce the undesirable destructive effect and prevent metal dissolution, the corrosion inhibitors were used³. The inhibition efficiency

of the inhibitors is largely depending on their adsorption on the metal surface³. Most well-known inhibitors are organic compounds containing hetero-atoms such as nitrogen, sulphur, and/or oxygen atoms^{4,5}. In addition, many N-heterocyclic compounds have been demonstrated as effective inhibitors against metals corrosion in acidic solutions⁶⁻⁸. The use of these organic compounds as inhibitors is one of the most used methods for protecting materials from corrosion^{9,10}. Recently, many researches have reoriented their attention to the development of new organic corrosion inhibitors such as imidazopyridine¹¹, imidazole^{12,13}, triazepine carboxylate¹⁴, and tetrazole^{15,16}. So, the majority of these organic compounds act via adsorption on the metal surface; where their adsorption depend mainly on certain physicochemical properties of the inhibitor molecule such as functional groups, steric factors, aromaticity, electron density at the donor atoms and π orbital character of donating electrons^{17,18}, the electronic molecular structure^{19,20}, and so on.

*e-mail: omarfergachi@yahoo.fr

In this study, the inhibition efficiency effect of two new imidazole derivatives, namely, phenyl (2-(3,4,5-trimethoxyphenyl)-1H-benzo [d] imidazol-1-yl) methanone called (P3) and (2-(4-methoxyphenyl)-1H-benzo [d] imidazol-1-yl) (phenyl) methanone called (P4) on ordinary steel in 5 M hydrochloric acid solution was investigated by using electrochemical measurements, theoretical study, SEM/EDX analyses and UV-Vis spectroscopy. Also, the adsorption behaviour of these series and the effect of temperature solution on their performance were examined.

2. Experimental Procedure

2.1. Synthesis of inhibitors

The 0.01 mol of O-phenylenediamine and 0.01 mol of benzoic acid were heated in a sealed tube with 10 mL of 20% hydrochloric acid for 4 hours at 418-423 K. After this, the neutralization of the reaction mixture gave a small amount, which 6% raw product recrystallization from aqueous ethanol to give colorless products. Their molecular structures are presented in Figure 1.

2.2. Materials

The corrosion tests were performed on ordinary steel; where its chemical composition is presented in Table 1 (the rest is ordinary steel balance).

For the electrochemical measurements and surface analyses, the used ordinary steel specimens were prepared by polishing with emery paper at different grit sizes (from 60 to 1200), rinsing with distilled water, degreasing in ethanol, and drying at hot air. The aggressive solution of 5.0 M HCl was prepared by dilution of analytical grade 35% HCl with distilled water.

2.3. Electrochemical cell and methods

2.3.1. Potentiodynamic polarization measurement

For this study, the working electrode was immersed in corrosive solution during 30 minutes to obtain a steady state of open circuit potential (Eocp). After this, the potentiodynamic polarization curve was recorded by polarization from the negative direction, under potentiodynamic conditions corresponding

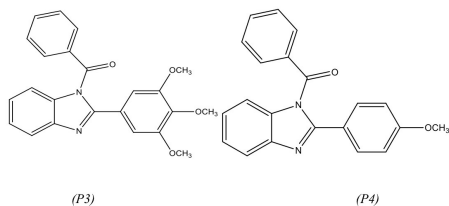


Figure 1. Molecular structure of phenyl (2-(3,4,5-trimethoxyphenyl)-1H-benzo[d]imidazol-1-yl) methanone (P3) and (2-(4-methoxyphenyl)-1H-benzo[d]imidazol-1-yl) (phenyl) methanone (P4).

to 1 mV/s (sweep rate) and under air atmosphere, to positive direction using a VoltaLab PGZ 100, which was controlled by a personal computer.

The corrosion kinetic parameters were determined by a fitting using Stern-Geary equation²¹; and the inhibition efficiency was calculated by the relationship:

$$\eta_{PP} = \frac{i_{corr}^0 - i_{corr}}{i_{corr}^0} \times 100 \quad (1)$$

Where i_{corr}^0 and i_{corr} are the corrosion current densities values without and with inhibitor, respectively.

2.3.2. Electrochemical impedance spectroscopy measurements (EIS)

The electrochemical impedance spectroscopy measurements were carried out using a transfer function analyzer (VoltaLab PGZ 100), with a small amplitude ac. Signal (10 mV.rms), over a frequency domain from 100 KHz to 10 mHz at 298 K and an air atmosphere. The results were then analyzed in terms of equivalent electrical circuit using Z-View software like as previously²²; and the inhibition efficiency was determined using the relationship:

$$\eta_{EIS} = \frac{R_{ct} - R_{ct}^0}{R_{ct}} \times 100 \quad (2)$$

Where R_{ct}^0 and R_{ct} are the transfer resistance values in the absence and the presence of inhibitor, respectively.

2.4. Quantum chemical calculations

In order to establish the relationship between the molecular structure and the obtained inhibition efficiency and to highlight the descriptors which are the best to describe these corrosion inhibition character, the quantum study have been adopted by the DFT (B3LYP) method using the 6-31G basis (d, p), where the calculation is done using a Gaussian software 09W²³⁻²⁵. The geometric optimization of P3 and P4 was carried out in the gaseous phase.

The following equations express the various molecular quantum parameters such as electronegativity (χ), electronic affinity (A), ionization potential (I) and gap energy (ΔE_{gap})²⁶⁻²⁹:

$$\Delta E_{gap} = E_{LUMO} - E_{HOMO} \quad (3)$$

$$I = -E_{HOMO} \quad (4)$$

$$A = -E_{LUMO} \quad (5)$$

$$\chi = \frac{I + A}{2} \quad (6)$$

Where E_{HOMO} is the energy of the highest occupied molecular orbital and E_{LUMO} is the energy of the lowest vacant molecular orbital.

Table 1. Chemical composition of ordinary steel sample.

Elements	C	Si	Mn	Cr	Mo	Ni	Al	Cu	Co	V	W
Percentage (wt. %)	0.11	0.24	0.47	0.12	0.02	0.10	0.03	0.14	< 0.0012	< 0.003	0.06

However, the overall hardness (η) and the chemical softness (σ) are given as follows³⁰:

$$\eta = \frac{\Delta E_{gap}}{2} \quad (7)$$

$$\sigma = \frac{1}{\eta} \quad (8)$$

The global electrophile index (ω) was introduced by Parr³¹ and is given by:

$$\omega = \frac{\mu^2}{2\eta} \quad (9)$$

Where μ is the electronic chemical potential, and obtained as follows: $\mu = -\chi^2$. This index measures the propensity of chemical species to accept electrons. Thus, a good more reactive nucleophile was characterized by a lower value of μ and ω .

On the other hand, the transferred electrons number (ΔN) was calculated as follows³²:

$$\Delta N = \frac{\chi_{Fe} - \chi_{inh}}{2(\eta_{Fe} + \eta_{inh})} \quad (10)$$

Where the $\chi_{Fe} = 7.0$ eV and $\eta_{Fe} = 0$ eV represent respectively the absolute electronegativity of iron and the molecule inhibitor³³. The η_{Fe} and η_{inh} denote respectively the absolute hardness of iron and the inhibitor molecule.

2.5. UV-visible spectrophotometer

In order to characterize the free solution and inhibited after six days of immersion at 298 K, the spectro-photometric method was carried out in 10^{-3} M of each inhibitor with 5.0 M HCl solution without and with ordinary steel sample by using a Beckman DU640 UV/Vis spectrophotometer.

2.6. Surface analysis

The morphology and the chemical composition the ordinary steel surface were obtained by the scanning electron

microscopy (SEM) instrument coupled with Energy Dispersive Spectroscopy (EDX) (SEM, JOEL JSM-5500) at 10 keV with magnification (800 \times) after 24 hours of immersion in 5.0 M HCl solution at 298 K without and with 10^{-3} M of each inhibitor.

3. Results and Discussion

3.1. Potentiodynamic polarization measurement

Figure 2 shows the Tafel polarization curves for ordinary steel in 5.0 M HCl in the absence and presence of different concentrations of P3 or P4 at 298 K. Their extracted electrochemical parameters, such as the corrosion potential E_{corr} , the cathodic and anodic Tafel slopes β_c and β_a , the corrosion current density i_{corr} , and the inhibition efficiency values η_{pp} (%) are determined from polarization curves and presented in Table 2. It is clear that i_{corr} values decrease sharply with the presence of P3 or P4. Correspondingly, the η_{pp} (%) values increase with inhibitor concentration to reach a maximum of 97.0% and 91.7% at 10^{-3} M for P3 and P4, respectively. These values suggested that two compounds act as effective inhibitors for ordinary steel corrosion in 5.0 M HCl solution. In addition, it is noted that these compounds act as mixed type inhibitors. On the other hand, it is remarked that the cathodic Tafel slopes generally unchanged with an increase of P3 and P4 concentrations; indicating that the inhibitors addition does not alter the hydrogen reaction mechanism³⁴. For the same, the obtained anodic Tafel slopes indicated that the P3 and P4 addition changes the anodic dissolution of ordinary steel.

3.2. Electrochemical impedance spectroscopy

The obtained Nyquist diagrams for ordinary steel in uninhibited and inhibited 5.0 M HCl solution are shown in Figure 3. The electrochemical parameters derived from these diagrams and the calculated inhibition efficiency values are presented in Table 3. It is noted that all impedance

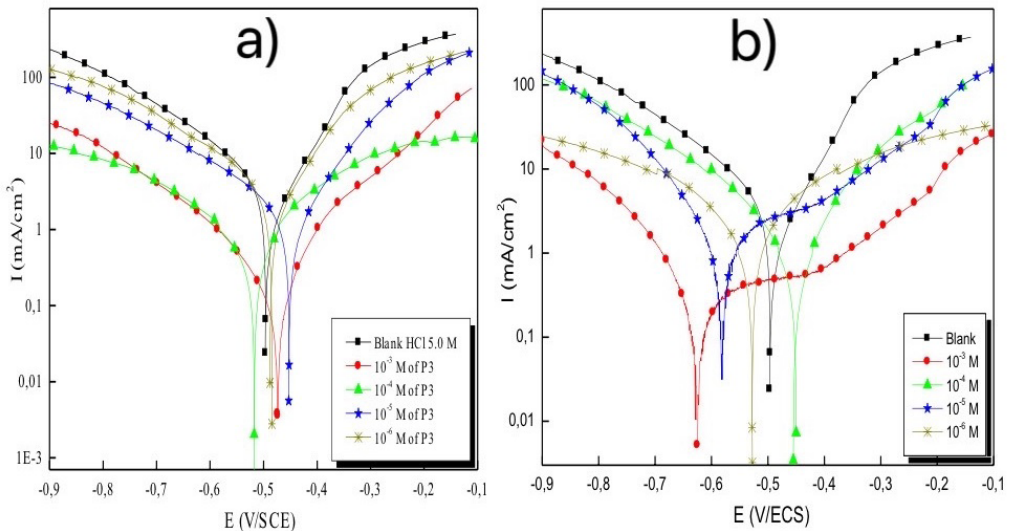


Figure 2. Tafel polarization curves for ordinary mild steel obtained in 5.0 M HCl solution containing different concentrations at 298 K of (a) P3 or (b) P4.

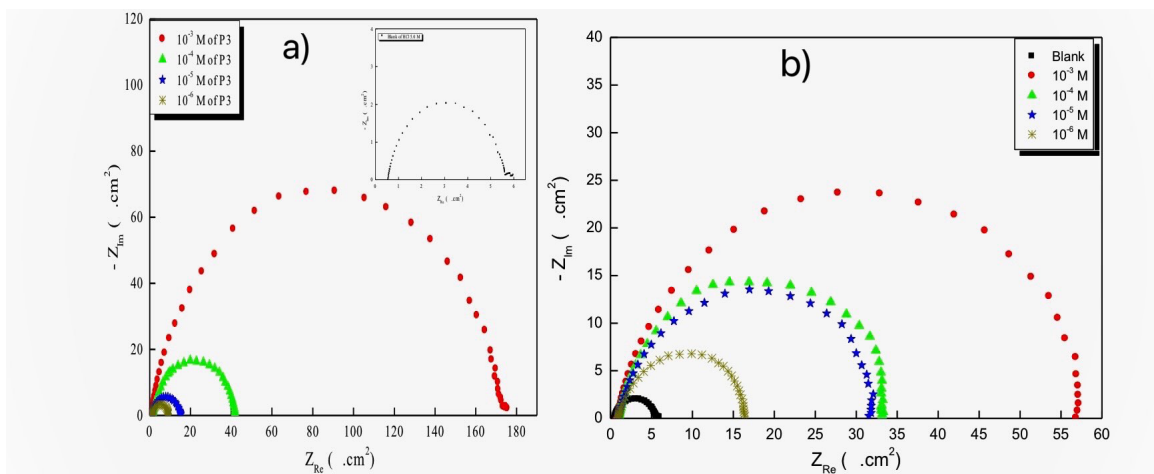


Figure 3. Nyquist impedance diagrams for ordinary mild steel in 5.0 M HCl solution at 298 K containing different concentrations of (a) P3 or (b) P4.

Table 2. Electrochemical parameters and inhibition efficiency values for ordinary steel in 5.0 M HCl solution without and with P3 or P4 addition at different concentrations.

Compounds	C	E_{corr} mV/SCE	i_{corr} $\mu\text{A cm}^{-2}$	β_x mV dec ⁻¹	β_a mV dec ⁻¹	Θ	η_{pp} %
	M						
5.0 M HCl	0	-494	4429	-202	92	-	-
P 3	10^{-3}	-472	130	-169	127	0.97	97.0
	10^{-4}	-516	520	-174	117	0.882	88.2
	10^{-5}	-449	1578	-180	118	0.643	64.3
	10^{-6}	-483	2731	-188	111	0.383	38.3
P 4	10^{-3}	-625	385	-159	120	0.913	91.3
	10^{-4}	-450	671	-177	114	0.848	84.8
	10^{-5}	-580	685	-139	115	0.845	84.5
	10^{-6}	-525	1277	-155	124	0.711	71.1

Table 3. Electrochemical impedance parameters and inhibition efficiency values for ordinary steel in 5.0 M HCl solution without and with P3 or P4 addition at different concentrations.

	C	R_s	R_{ct}	Q_{dl}	n_{dl}	C_{dl}	η_{EIS} %
	M	$\Omega \text{ cm}^2$	$\Omega \text{ cm}^2$	$\mu\text{F S}^{-1}$		$\mu\text{F cm}^{-2}$	
5.0 M HCl	00	0.55	5	359	0.858	127	-
P3	10^{-3}	0.88	173.4	60.5	0.852	27.5	97.1
	10^{-4}	1.32	41.17	149.5	0.841	47.02	87.8
	10^{-5}	0.87	14.47	215.4	0.834	84.38	65.4
	10^{-6}	1.13	8.10	218.1	0.901	109.1	38.3
P4	10^{-3}	0.87	57	104	0.892	52.8	91.2
	10^{-4}	0.95	32.7	137	0.885	73.2	84.7
	10^{-5}	0.92	32.2	219	0.862	99.6	84.4
	10^{-6}	0.87	16.9	360	0.845	142	70.4

spectra have a single capacitive loop, which suggests that the ordinary steel corrosion process in 5.0 M HCl with and without inhibitors is mainly controlled by a charge transfer process³⁵. Moreover, these diagrams are mainly similar for all tested concentrations, indicating that there is virtually no change in the corrosion mechanism³⁶. In addition, these Nyquist diagrams are not perfect semicircles, which can be attributed to the frequency dispersion of the interfacial

impedance³⁷, and/or due to the surface roughness, the chemical heterogeneity of the surface, and the adsorption-desorption process of molecules inhibitors on ordinary steel surface³⁸. On the other hand, it is observed that the semicircles diameter increase with the presence of P3 or P4, which may be related to the increase in surface coverage of the ordinary steel by the molecules inhibitors. In order to extract the EIS data the proposed equivalent circuit shown in Figure 4 was used. Thus,

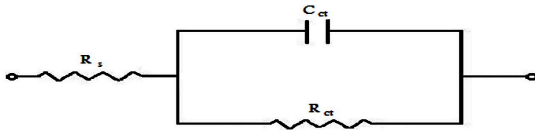


Figure 4. Proposal electrical equivalent circuit used for metal/solution interface.

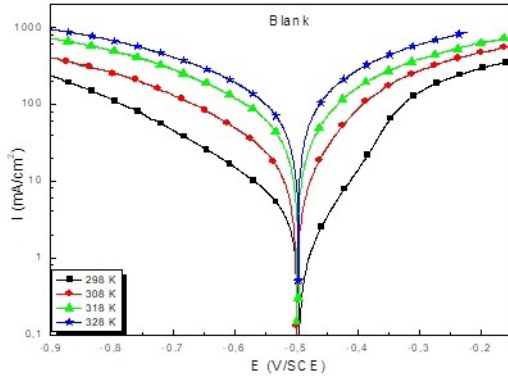


Figure 5. Potentiodynamic polarization curves for ordinary mild steel in 5.0 M HCl solution in the absence of inhibitors at different temperatures range.

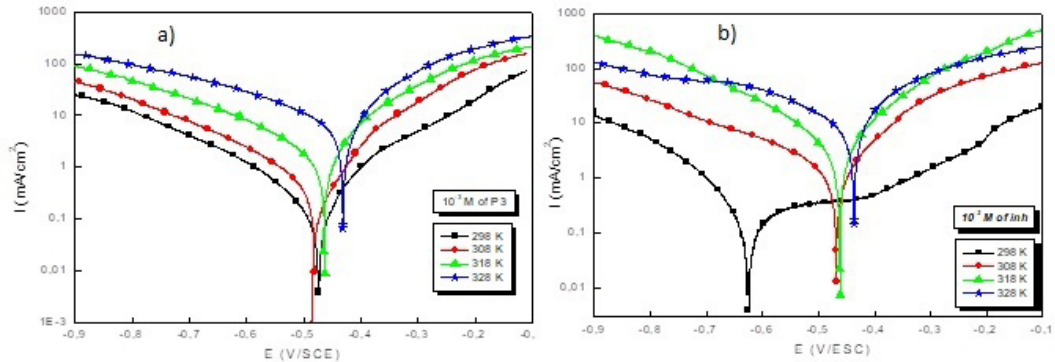


Figure 6. Potentiodynamic polarization curves for ordinary mild steel in 5.0 M HCl with the presence of 10^{-3} M of (a) P3 or (b) P4 at different temperatures range.

Table 4. Electrochemical parameters and inhibition efficiency values obtained for ordinary steel in 5.0 M HCl without and with 10^{-3} M of P3 and P4.

	T	E_{corr} mV/SCE	i_{corr} $\mu\text{A}/\text{cm}^2$	β_c	β_a	η_{pp}
	K					
Blank solution	298	-494	4429	-202	92	-
	308	-499	6213	-189	99	-
	318	-497	9179	-175	122	-
	328	-496	16923	-156	132	-
10^{-3} M of P3	298	-472	130	-169	127	97.0
	308	-477	325	-185	117	94.7
	318	-458	764	-188	111	91.6
	328	-428	2016	-194	105	88.0
10^{-3} M of P4	298	-625	385	-159	120	91.3
	308	-464	675	-155	116	89.1
	318	-460	1198	-158	124	86.9
	328	-434	2543	-159	127	84.9

the CPE element was used to explain the depression of the capacitance semicircle, corresponding to many properties like the above. This element is represented by the following expression^{39,40}:

$$Z_{\text{CPE}} = \frac{1}{Q(j\omega)^{ndl}} \quad (11)$$

3.3. Effect of solution temperature

To calculate the activation and thermodynamic parameters of corrosion process and study the mechanism action of inhibitors, the effect of solution temperature on the inhibition efficiency of P3 and P4 for ordinary steel 5.0 M HCl was studied at the temperature range from 298 K to 328 K. The obtained potentiodynamic polarization curves for ordinary steel in 5.0 M HCl in the absence and the presence of 10^{-3} M of P3 or P4, are presented in Figures 5 and 6. Their extracted electrochemical parameters and the calculated inhibition efficiency are illustrated in Table 4. It is clear that the current density values increase and the η_{pp} % inhibition efficiency values decrease slightly with the increase of the temperature. These findings were attributed to the increase of the kinetic energy and/or the decrease in the adsorption capacity of the organic compounds at high temperature⁴¹.

However, the activation and transition parameters of the corrosion process were calculated from an Arrhenius and transition curves according to the following equations⁴²:

$$i_{corr} = A \exp\left(-\frac{E_a}{RT}\right) \quad (12)$$

$$i_{corr} = \frac{RT}{Nh} \exp\left(\frac{\Delta S_a}{R}\right) \exp\left(\frac{\Delta H_a}{RT}\right) \quad (13)$$

Where E_a is the apparent activation energy, A is the Arrhenius factor, h is the plank constant, N is the Avogadro number, ΔH_a and ΔS_a are the enthalpy and entropy energies, and R is the gas constant.

On the other hand, the apparent activation energy was determined from the $\ln(i_{corr}) = f(1/T)$ curves (Figure 7), and the ΔH_a and ΔS_a values were determined from $\ln(i_{corr}/T) = f(1/T)$ (Figure 8). These parameters were listed in Table 5. It is observed that all the obtained values in the presence of P3 or P4 are higher than their absence. In fact, the value of ΔH_a for the dissolution reaction of ordinary steel in 5.0 M HCl in the presence of P3 is higher than in the presence of P4 and in the blank solution. These results reflect the endothermic

nature of the ordinary steel dissolution process, which also due to the positive sign of enthalpy^{43,44}.

However, a higher energy barrier for the corrosion process in the presence of inhibitors was associated with physical adsorption or low chemical bond between the inhibitors molecules and the ordinary steel surface^{45,46}, whereas unchanged or lower activation energy in the presence of inhibitors suggests chemisorption⁴⁷. So, in this study, it is found that the E_a value increases with the presence of inhibitors, which can be interpreted as physical adsorption. In addition, this increase can be attributed to the decrease of the inhibitor molecules adsorption on the metallic surface with the rise of temperature⁴⁸. In this context, the increase in temperature led to an increase in the electron density of the adsorption centers, which improved the inhibition efficiency⁴⁹.

Beyond that, Table 5 showed that the ΔS_a value in the presence of inhibitors is lower compared to blank solution. This phenomenon suggested that a decrease in randomness occurred between the transitions of reagents to the activated complex. Additionally, the obtained negative values of ΔS_a for P4 indicated that the activated complex in the velocity determination step is an association rather than dissociation

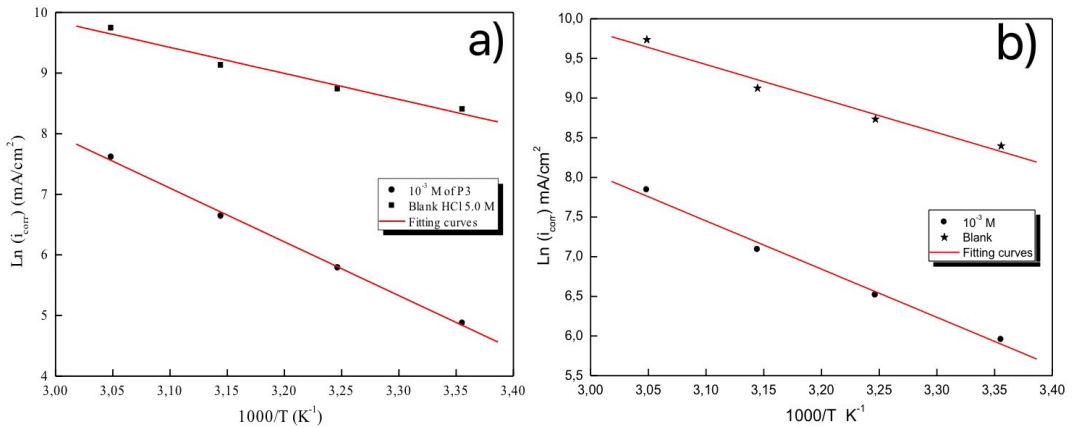


Figure 7. Arrhenius plots of ordinary mild steel in 5.0 M HCl without and with 10⁻³ M of (a) P3 or (b) P4.

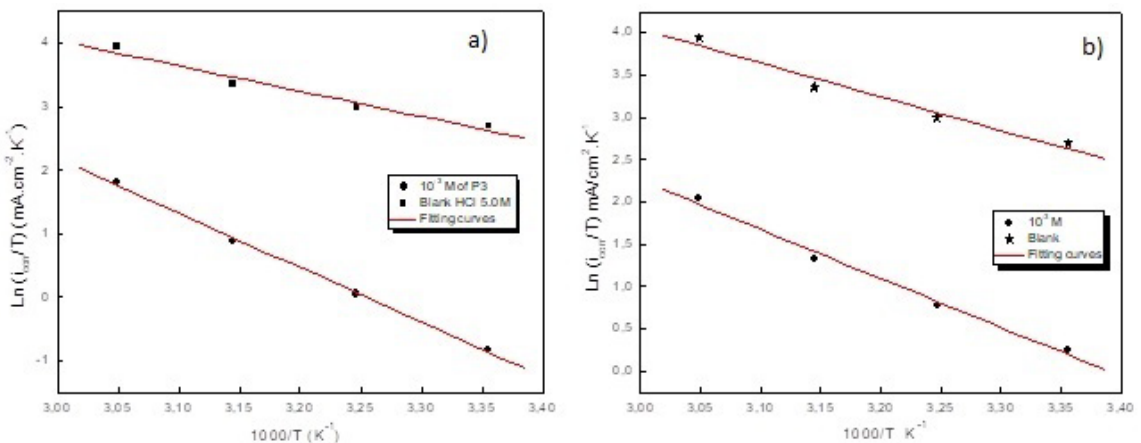


Figure 8. Transition Arrhenius plots of ordinary mild steel in 5.0 M HCl without and with 10⁻³ M of (a) P3 or (b) P4.

step, which means that a decrease in disorder occurs, when substituting reactants to the activated complex^{50,51}.

3.4. Adsorption isotherm

The adsorption isotherm describing the adsorption behaviour of organic inhibitors is important for knowing the corrosion inhibition mechanism. They can provide basic information about the interactions between inhibitor molecules and the metal surface. Thus, several adsorption isotherms have been tested to adapt the surface coverage degree (θ) to adsorption isotherms, including Frumkin, Temkin, Freundlich, and Langmuir isotherms⁵². It is found that the plot C_{inh}/θ against C_{inh} (Figure 9) gives a straight line with a correlation coefficient of 0.999 for both inhibitors, providing that their adsorption on the ordinary steel surface obeys the Langmuir adsorption isotherm. This isotherm can be represented by⁵³:

$$\frac{C_{inh}}{\theta} = \frac{1}{K_{ads}} + C_{inh} \quad (14)$$

Where C_{inh} is the concentration of the used inhibitor (mol L^{-1}) and K_{ads} is the equilibrium constant for the adsorption and the desorption process, which is linked to the free energy of the adsorption (ΔG_{ads})⁵⁴:

Table 5. Values of activation and thermodynamic parameters for ordinary steel in 5.0 M HCl without and with 10^{-3} M of P3 or P4.

	E_a (KJ/mol)	ΔH_a (KJ/mol)	ΔS_a (KJ/mol K)
Blank solution	35.68	33.09	-64.64
10^{-3} M of P3	73.70	71.10	33.91
10^{-3} M of P4	50.55	47.95	-34.94

Table 6. Calculated parameters of the adsorption of P3 and P4 on ordinary steel surface.

Interface	R^2	K_{ads} (L/mol)	ΔG_{ads} (KJ/mol)
ordinary steel/5.0 M HCl/P3	0.99997	$17.45 \cdot 10^4$	-39.85
ordinary steel/5.0 M HCl/P4	0.99997	$32.09 \cdot 10^4$	-41.36

$$K_{ads} = \frac{1}{55.55} \exp\left(\frac{-\Delta G_{ads}}{RT}\right) \quad (15)$$

Where R is the constant of universal gas, 55.55 is the water concentration in solution (mol L^{-1}), and T is the absolute temperature (K).

It is found that the K_{ads} values are about $17.45 \cdot 10^4$ L/mol, and $32.09 \cdot 10^4$ L/mol for P3 and P4, respectively (Table 6). These high values reflect the high adsorption capacity of inhibitors on ordinary steel surface⁵⁵.

Additionally, it is obtained that the ΔG_{ads} values are -39.85 kJ mol^{-1} and -41.36 kJ mol^{-1} for P3 and P4, respectively. The negative values of these parameters indicate the spontaneity of the adsorption process and the stability of the adsorbed layer on the ordinary steel surface. In addition, it is well known that when the ΔG_{ads} value is about -20 kJ mol^{-1} or less indicates physisorption; those of the order of -40 kJ mol^{-1} or more involves chemisorption^{56,57}. On the other hand, the adsorption phenomenon of an organic molecule is not considered solely as a purely physical or chemical adsorption phenomenon^{58,59}. In our case, the obtained values of ΔG_{ads} may suggest chemisorption and physisorption modes for both compounds P3 and P4.

3.5. UV-visible spectroscopy

In order to confirm the possibility of formation of P3-Fe and P4-Fe complexes, the UV-Visible absorption analyses was used for ordinary steel in 5.0 M HCl solution containing 10^{-3} M of P3 or P4 before and after 6 days of immersion. The obtained spectra are shown in Figure 10. The obtained figures show a difference between absorbance values and their intensities with the presence of inhibitors. It is noted that the absorbance increases after immersion of ordinary steel in the solution containing P3 or P4. This finding reveals the formation of a complex between Fe^{2+} ions and inhibitor molecules. The formation of this complex may be responsible for the observed deviation of absorbance and its intensity value⁶⁰. The electron absorption spectrum of P3 and P4 solutions prior to ordinary steel immersion has a

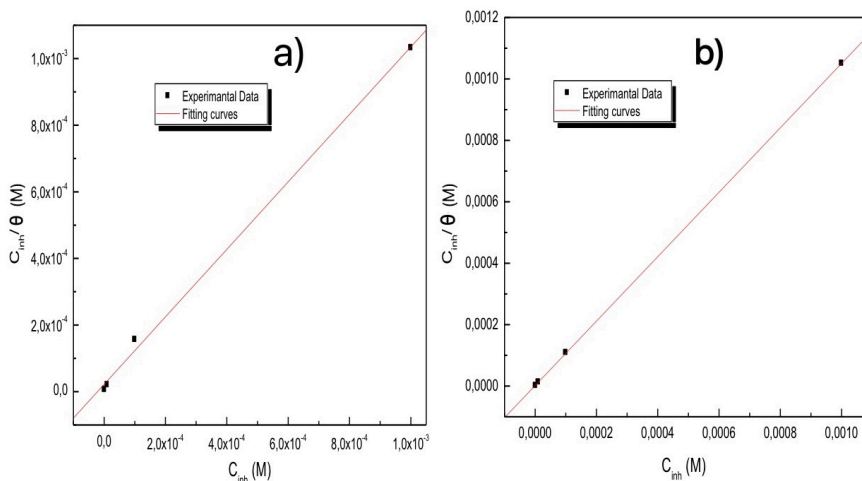


Figure 9. Langmuir isotherm adsorption curves for (a) P3 and (b) P4.

main visible absorption band between 200 nm and 350 nm, with a corresponding absorbance of 3.0; and between 200 nm and 380 nm with an absorbance of 3.0. This band can be assigned to the $\pi-\pi^*$ transition, involving the entire electronic structure system of compounds with charge transfer character⁶¹. After six days of ordinary steel immersion, the absorption band (λ_{\max}) of P3 and P4 underwent a red shift of 350–400 nm and 380–420 nm, suggesting an interaction between inhibitors molecules and Fe^{2+} ions in solution^{62,63}. These experimental findings are strong evidence of the possibility of the formation of iron-inhibitor complex. It should also be noted that there are no significant difference of the spectrum for P3 before and after immersion of ordinary steel, showing a possibility of weak interaction between it

and P3 molecules (physisorption)⁶⁴, confirming the obtained value of free energy calculated from adsorption isotherm.

3.6. SEM micrographs and EDX characterization

The SEM micrographs of the ordinary mild steel surface in 5.0 M HCl medium after 24 hours of immersion time and at 298 K in the absence and presence of 10⁻³ M of P3 or P4 were presented in Figure 11. The observation of the micrograph of ordinary mild steel in the acidic solution without inhibitors showed that the state surface was intensely damaged, due to quick corrosion degradation with the presence of the pitted areas (Figure 11a). This last form is typical to pitting corrosion⁶⁵. On the other hand, in the presence of 10⁻³ M of P3 (Figure 11b) or P4 (Figure 11c),

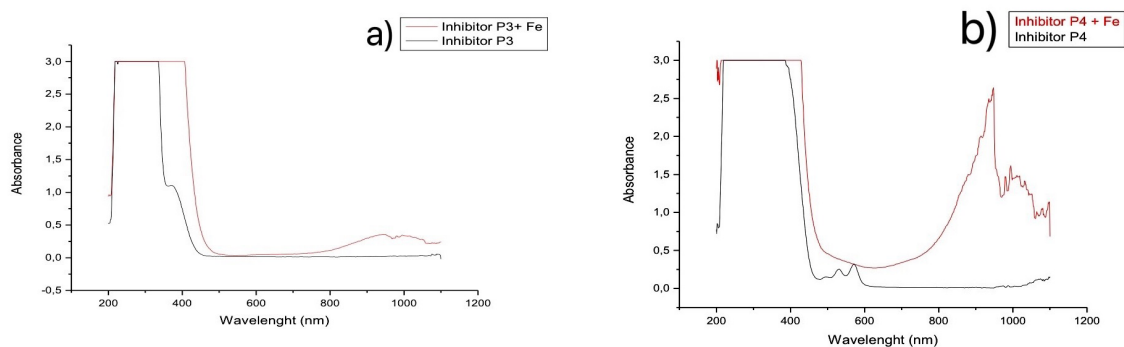


Figure 10. UV-visible spectra obtained for 5.0 M HCl solution containing 10⁻³ M of (a) P3 or (b) P4 before (Black) and after (Red) 6 days of immersion of ordinary mild steel.

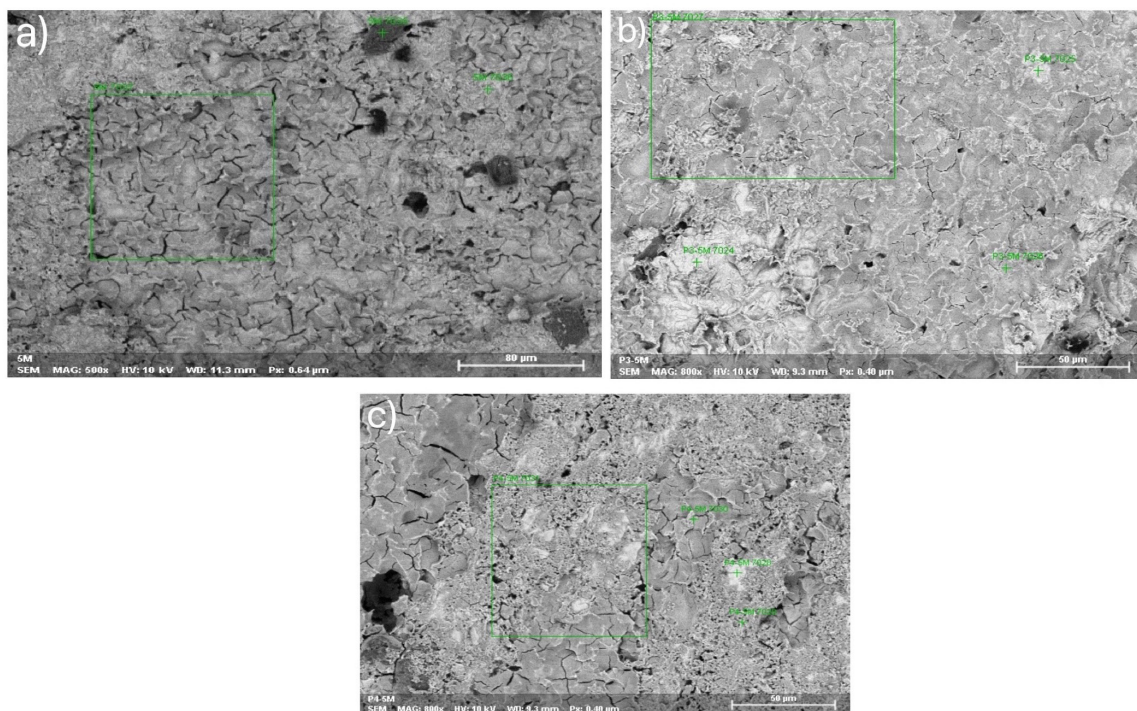


Figure 11. SEM micrograph for ordinary mild steel surface after 24 h of immersion in 5.0 M HCl solution (a) blank solution, (b) with the presence of 10⁻³ M of P3 and (c) with the presence of 10⁻³ M of P4.

it is observed that the surface is smooth and covered with the presence of the traces in the form of a plate, indicating the presence of the organic products. This remark showed that the corrosion protection is due to the formation of a deposit by the formation of a film of the molecule inhibitors on ordinary mild steel surface⁶⁶. In addition, it is observed that the pitting areas disappear and the ordinary mild steel surface is almost free of corrosion products with the presence of P3 or P4.

After studying the morphology of ordinary mild steel surface, its chemical composition was examined by EDX analyses. These EDX analyses at different zones reveal the presence of nitrogen, molybdenum, carbon, oxygen and chlorine atoms (Figure 12). For the blank solution, the presence of oxygen and iron atoms suggests the presence of corrosion products composed of iron hydroxide and/or oxide (Figure 12a). On the other hand, the presence of nitrogen and carbon testifies to the adsorption of inhibitors molecules on the ordinary mild steel surface. It is noted that the oxygen peak is much larger in the presence of P3 (Figure 12b) or P4 (Figure 12c), which is certainly due to their adsorption on the metallic surface. The presence of Cl atom suggested that the formed film by inhibitors blocks the attack by chloride ions, which accumulate on the film surface. In addition, in the construction of the inhibitory film, the presence of iron on the EDX spectrum can also be explained by the complex formation between the P3 or P4 molecules and the Fe²⁺ ions resulting from the iron dissolution.

3.7. Chemical quantum calculations

To be able to study the effect of the molecular structure on the inhibition efficiency of P3 and P4, quantum calculations

have been made using the DFT. The optimized geometry, HOMO and LUMO orbitals for P3 and P4 in gaseous media, are shown in Figures 13 and 14. The quantum chemical parameters calculated at the B3LYP / 6-31 (d, p) level for the neutral and protonated forms of P3 and P4 compounds are illustrated in Table 7. In general, the increase of EHOMO value and the decrease of ELUMO value are related to the increase of the electron donation and acceptance capacity of the inhibitor to the vacant d-orbital of the metal and from the filled orbitals, respectively. In addition, the lower ΔE value designates the easier release of electrons, the stronger adsorption, the higher chemical activity, and kinetic stability^{67,68}. Thus, to become a good corrosion inhibitor, it is necessary to easily give electrons and easily accept them in vacant orbital of metal⁶⁹. It is found that the values of EHOMO follows the order: P4 > P3 for both neutral and protonated forms, suggesting the high inhibition efficiency observed for P4 due to its better potential to give electrons in its extreme molecular orbit an appropriate orbital in the metal atom compared to P3. In the same, the low ELUMO values tend to easily accept electrons⁷⁰. In fact, ELUMO for P3 is greater than P4 in protonated form, while it is almost equal in neutral form, suggesting that P3 is more willing to accept charges from metallic atomic orbitals. This parameter trend does not reflect the observed order of inhibition efficiency. In addition, the energy gap (ΔE) is often used to characterize the chemical reactivity and kinetic stability of molecules⁷¹. The obtained trend of ΔE follows the order: P4 < P3, implying that P4 is the most reactive inhibitor.

However, the overall chemical hardness (η) and flexibility (σ) have all been used as molecular descriptors of reactivity and selectivity⁷². In this concept, a hard molecule would

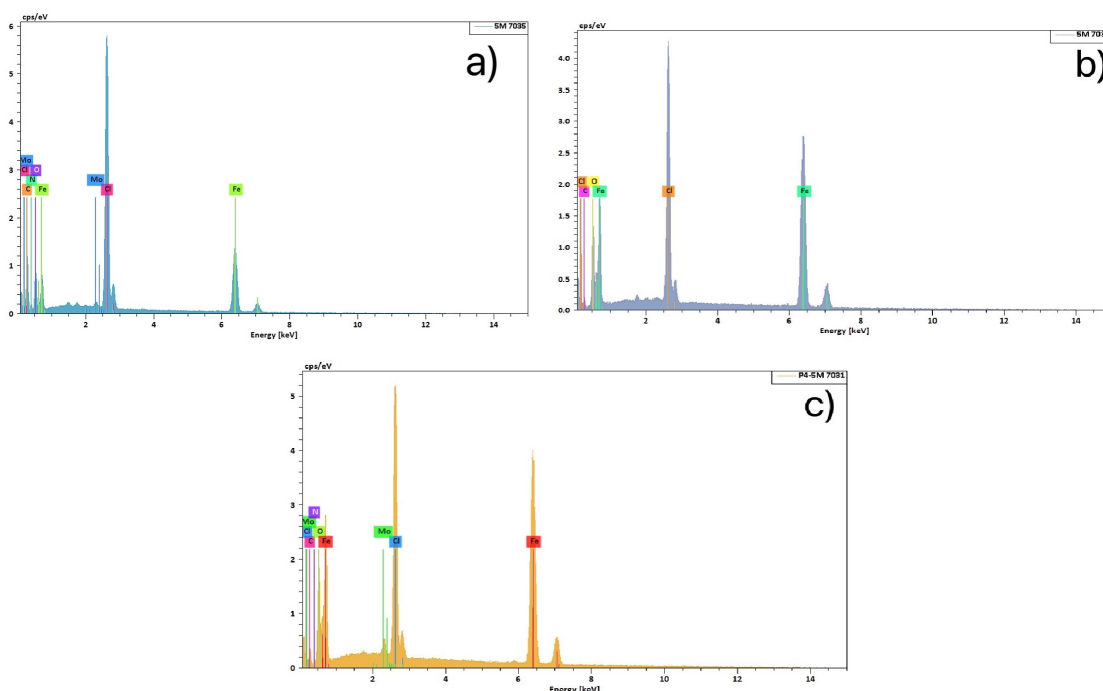


Figure 12. EDX spectra for ordinary mild steel surface after 24 h of immersion in 5.0 M HCl solution (a) blank solution, (b) with the presence of 10⁻³ M of P3, and (c) with the presence of 10⁻³ M of P4.

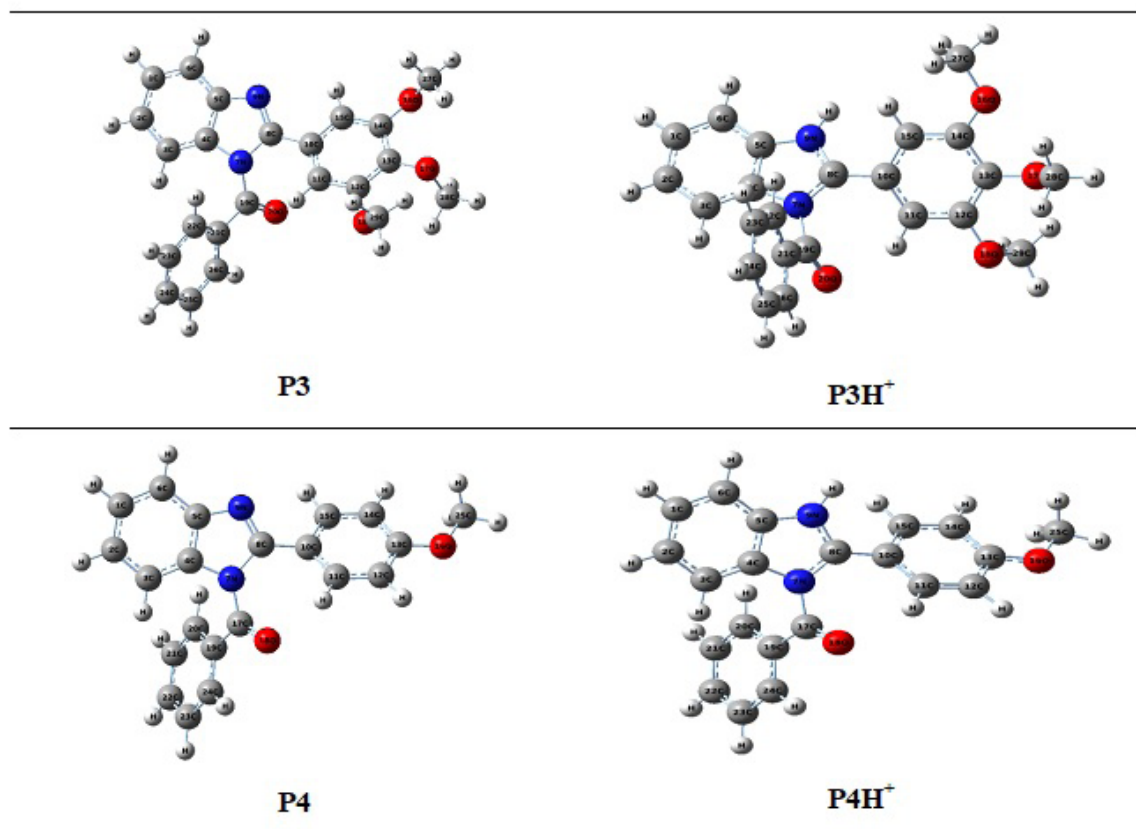


Figure 13. Optimized structures of neutral and protonated forms of P3 and P4 calculated by DFT with B3LYP / 6-31g (d, p).

Table 7. Quantum chemical parameters calculated at the B3LYP/6-31(d, p) level for the neutral and protonated forms of P3 and P4 compounds in gaseous and aqueous phases.

Parameters	Phases	Neutral forms		Protonated forms	
		P3	P4	P3H ⁺	P4H ⁺
E _{HOMO} (eV)	G	-5.7490	-5.5947	-6.0214	-9.2172
	A	-6.0318	-5.8100	-6.4824	-6.5327
E _{LUMO} (eV)	G	-1.9132	-1.9081	-2.2033	-5.3204
	A	-2.0360	-2.0106	-2.6488	-2.6156
ΔE(eV)	G	3.8358	3.6866	3.8181	3.8967
	A	3.9958	3.7993	3.8336	3.9171
μ(D)	G	4.1935	3.7081	9.8922	4.8470
	A	5.0431	3.6683	9.9686	6.9952
χ(eV)	G	3.8311	3.7514	4.1124	7.2688
	A	4.0339	3.9103	4.5656	4.5742
η(eV)	G	1.9179	1.8433	1.9090	1.9483
	A	1.9979	1.8996	1.9168	1.9585
σ (eV ⁻¹)	G	0.5214	0.5424	0.5238	0.5132
	A	0.5005	0.5264	0.5216	0.51057
ΔN	G	0.8261	0.8811	0.7562	-0.06899
	A	0.7423	0.8132	0.6350	0.61927

have a large ΔE value, while a soft molecule would have a small ΔE value (based on Lewis's theory of acid and bases and Pearson's concept of hard and soft acids and bases).

The order between structures based on σ values is P4 < P3 in protonated form and the inverse in the neutral form (adsorption usually occurs at the region of the molecule, where σ has

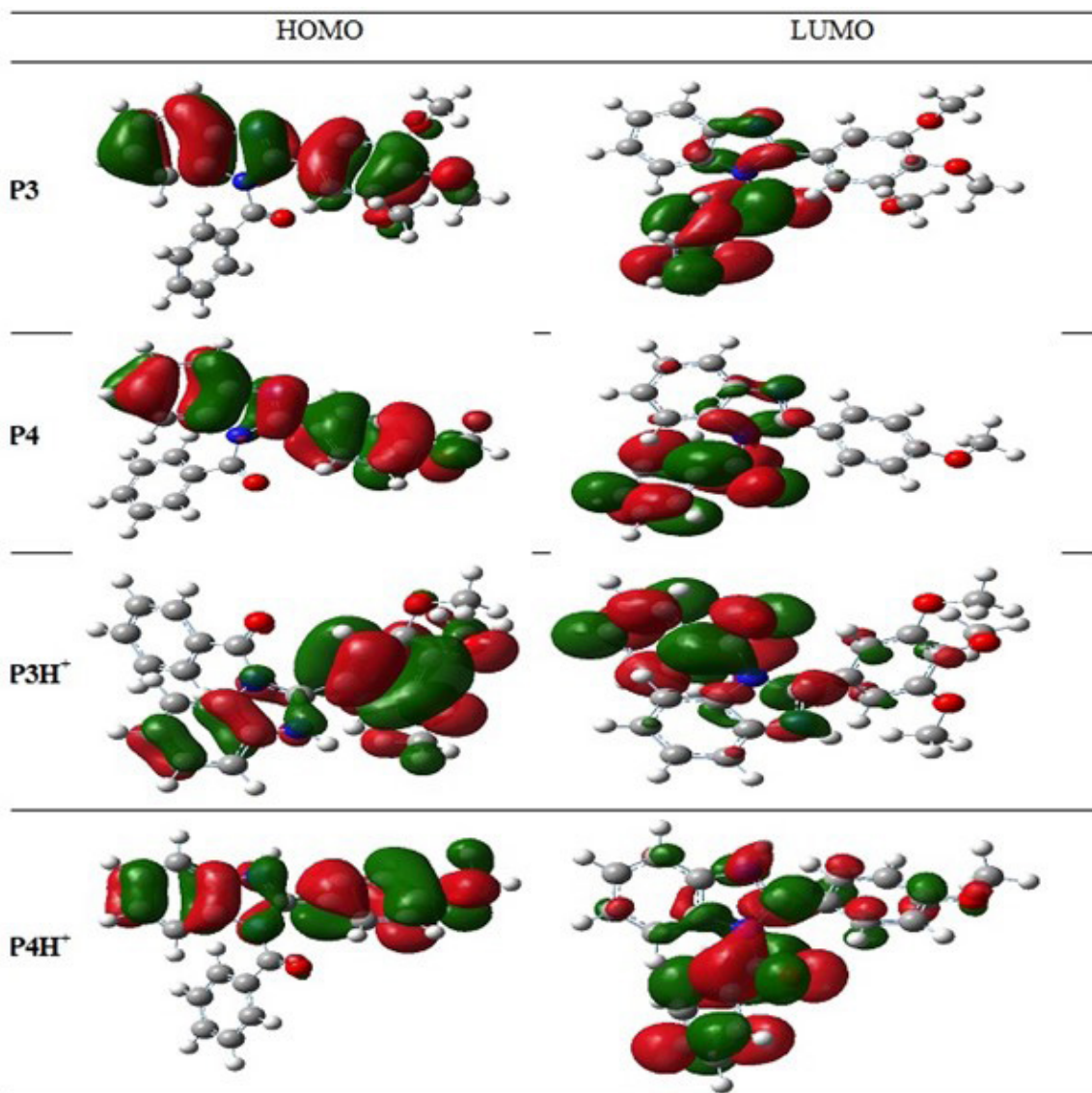


Figure 14. HOMO and LUMO boundary molecular orbitals for the neutral and protonated forms of P3 and P4.

the highest value)⁷³. Additionally, the electronegativity (χ) is often described as the negative of the potential of global electronic chemistry⁷⁴. The lowest χ value for P3H⁺ suggests that it tends to release its loosely bound electrons more easily than P4H⁺. This improves the best adsorption and inhibition activity⁷⁵. On the other hand, there is an opinion that a low dipole moment promotes high inhibition efficiency, and the accumulation of inhibitor molecules on the metal surface⁷⁶. However, no general trend of relationship exists between the dipole moments of P3 and P4 with the experimental inhibition efficiency. So, even though P4 with the least dipole moment had the lowest inhibition efficiency, while P3 with significantly high inhibition efficiency was found to have a higher dipole moment. This observation is somewhat in agreement with the hypothesis that a high moment improves the dipole-dipole interactions between

the inhibitor molecules and the charged metal surface; and thus promotes the performance inhibition^{77,78}.

4. Conclusion

In this study, two imidazole derivatives, namely : phenyl (2- (3,4,5 trimethoxyphenyl) -1H-benzo [d] imidazol-1-yl) methanone (P3) and (2- (4 -methoxyphenyl) -1H-benzo [d] imidazol-1-yl) (phenyl) methanone (P4) on the ordinary steel corrosion in 5.0 M HCl solution was investigated by using electrochemical measurements, scanning electron spectroscopy (SEM) coupled with Energy Dispersive Spectroscopy (EDX), UV-visible spectroscopy and theoretical study; and the principal important conclusions are:

- P3 and P4 compounds retard ordinary steel dissolution in 5.0 HCl solution, where their inhibition efficiency depends on the type of methoxy group

in their structures; and therefore they improve the corrosion resistance of ordinary steel in a pickling solution with HCl.

- The potentiodynamic polarization curves indicated that all compounds react as mixed-type inhibitor, and their η_{pp} % depend on their concentrations, which confirmed by EIS results.
- The obtained results showed that P3 had better corrosion inhibition efficiency for ordinary steel in 5.0 M HCl than that of P4. This higher inhibition efficiency of P3 was attributed the great number of $-OCH_3$ groups (three methoxy groups) presented in P3 structure.
- The inhibition efficiency of P3 and P4 decreases slightly with temperature, and their adsorption on ordinary steel surface was spontaneous, and labeled by electrostatic interactions.
- The adsorption of P3 and P4 molecules on ordinary steel surface obeys to the Langmuir adsorption isotherm.
- SEM analysis of the surface indicated the formation of a protective layer on ordinary steel surface and the UV-visible spectroscopy of the solution demonstrated the formation inhibitor-complex in solution.
- DFT calculation studies indicated that the electrons of aromatic rings, oxygen, and nitrogen heteroatoms were the major adsorption centers for strong donor/acceptor interactions with the unoccupied d-orbital of ordinary steel surface.

5. References

1. Koch G, Varney J, Thompson N, Moghissi O, Gould M, Payer J. International measures of prevention, application, and economics of corrosion technologies study. Houston: NACE International. 2016; 216 p.
2. Aouine Y, Sfaira M, Ebn Touhami M, Alami A, Hammouti B, Elbakri M, et al. Temperature and time investigations on the adsorption behavior of isoindoline, tetrazole and isoindoline-tetrazole on corrosion of mild steel in acidic medium. *Int J Electrochem Sci*. 2012;7:5400-19.
3. Tourir R, Dkhireche N, Ebn Touhami M, El Bakri M, Rochdi A, Belakhmima RA. Study of the mechanism action of sodium gluconate used for the protection of scale and corrosion in cooling water system. *J Saudi Chem Soc*. 2014;18:873-81.
4. Doubi M, About S, Erramli H, Dermaj A, Chebabe D, Tourir R, et al. Performance of the novel corrosion inhibitor based on Cetamine to protect mild steel in surface water solution: electrochemical and surface studies. *Chem Pap*. 2021;75(4):1679-90.
5. El-Sayed A. Phenothiazine as inhibitor of the corrosion of cadmium in acidic solutions. *J Appl Electrochem*. 1997;27(2):193-200.
6. Galai M, Rbaa M, Kacimi YE, Ouakki M, Dkhirech N, Tourir R, et al. Anti-corrosion properties of some triphenylim-idazole substituted compounds in corrosion inhibition of carbon steel in 1.0 M hydrochloric acid solution. *Anal Bioanal Electrochem*. 2017;9(1):80-101.
7. Barouni K, Kassale A, Albourine A, Jbara O, Hammouti B, Bazzi L. Amino acids as corrosion inhibitors for copper in nitric acid medium: experimental and theoretical study. *J Mater Environ Sci*. 2014;5(2):456-63.
8. Schmitt G. Application of inhibitors for acid media: report prepared for the European federation of corrosion working party on inhibitors. *Br Corros J*. 1984;19(4):165-76.
9. El-Rehim SA, Ibrahim MA, Khaled KF. 4-Aminoantipyrine as an inhibitor of mild steel corrosion in HCl solution. *J Appl Electrochem*. 1999;29(5):593-9.
10. Li XH, Deng SD, Fu H. Adsorption and inhibitive action of hexadecylpyridinium bromide on steel in phosphoric acid produced by dihydrate wet method process. *J Appl Electrochem*. 2011;41(5):507-17.
11. Ech-chihbi E, Belghiti ME, Salim R, Oudda H, Elaataoui A, Rais Z, et al. Effect of some imidazopyridine compounds on carbon steel corrosion in hydrochloric acid solution. *Pharma Chem*. 2016;8(13):214-30.
12. Ech-chihbi E, Belghiti ME, Salim R, Oudda H, Taleb M, Benchat N, et al. Experimental and computational studies on the inhibition performance of the organic compound "2-phenylimidazo [1,2-a]pyrimidine-3-carbaldehyde" against the corrosion of carbon steel in 1.0 M HCl solution. *Surf Interfaces*. 2017;9:206-17.
13. Dkhireche N, Galai M, Kacimi YE, Rbaa M, Ouakki M, Lakhrissi B, et al. New quinoline derivatives as sul-furic acid inhibitor's for mild steel. *Anal Bioanal Electrochem*. 2018;10(1):111-35.
14. Rbaa M, Galai M, El Kacimi Y, Ouakki M, Tourir R, Lakhrissi B, et al. Adsorption properties and inhibition of carbon steel corrosion in a hydrochloric solution by 2-(4,5-diphenyl-4,5-dihydro-1h-imidazol-2-yl) 5-methoxyphenol. *Electrochim Acta*. 2017;35(6):323-38.
15. Alaoui K, Tourir R, Galai M, Serrar H, Ouakki M, Kaya S, et al. Electrochemical and computational studies of some triazepine carboxylate compounds as acid corrosion inhibitors for mild steel. *J Bio Tribo Corr*. 2018;4(3):37.
16. Kertit S, Hammouti B. Corrosion inhibition of iron in 1 M HCl by 1-phenyl-5-mercapto-1,2,3,4-tetrazole. *Appl Surf Sci*. 1996;93(1):59-66.
17. Essoufi H, Kertit S, Hammout B, Benkaddour M. 1-Phe-nyl-5-mercapto 1,2,3,4-tetrazole (PMT) as corrosion inhibitor for nickel in sulphuric acid solution. *Bull Electrochem*. 2000;16(5):205-8.
18. Growcock FB, Frenier WW, Andreozzi PA. Inhibition of steel corrosion in HCl by derivatives of cinnamaldehyde: part II. Structure-activity correlations. *Corrosion*. 1989;45(12):1007-15.
19. Lukovits I, Kalman E, Palinkas G. Nonlinear group-contribution models of corrosion inhibition. *Corrosion*. 1995;51(3):201-5.
20. Bentiss F, Lagrenee M, Traisnel M, Memari B, Elattari H. A simple one step synthesis of new 3,5-disubstituted-4-amino-1,2,4-triazoles. *J Heterocycl Chem*. 1999;36(1):149-52.
21. Stern M, Geary AL. Electrochemical polarization I. A theoretical analysis of the shape of polarization curves. *J Electrochem Soc*. 1957;104(1):56-63.
22. Tourir R, Dkhireche N, Ebn Touhami M, Sfaira M, Senhaji O, Robin JJ, et al. Study of phosphonate addition and hydrodynamic conditions on ordinary steel corrosion inhibition in simulated cooling water. *Mater Chem Phys*. 2010;122:1-9.
23. Azaroual MA, El Harrak EF, Tourir R, Rochdi A, Ebn Touhami M. Synergistic corrosion protection for galvanized steel in 3.0% NaCl solution by sodium gluconate and cationic surfactant. *J Mol Liq*. 2016;220:549-57.
24. Frisch MJ, Trucks GW, Schlegel HB, Scuseria GE, Robb MA, Cheeseman JR, et al. Gaussian 03, Revision D. 03. Pittsburgh, PA: Gaussian; 2003.
25. Petersson GA, Bennett A, Tensfeldt TG, Al-Laham MA, Shirley WA, Mantzaris J. A complete basis set model chemistry. I. The total energies of closed-shell atoms and hydrides of the first-row elements. *J Chem Phys*. 1988;89:2193-218.
26. Ansari KR, Quraishi MA. Experimental and quantum chemical evaluation of Schiff bases of isatinasa new and green corrosion inhibitors for mild steel in 20% H2SO4. *J Aiwan Inst Chem Eng*. 2015;54:145-54.
27. Neese F. An Ab initio, DFT and Semiempirical SCF-MO Package Version 2.9. Mulheim an der Ruhr, Germany: Max Planck Institute for Bioinorganic Chemistry; 2012.

28. Becke DA. Density functional calculations of molecular bond energies. *J Chem Phys.* 1986;84:4524-9.
29. Lee C, Yang W, Parr GR. Development of the Colle-Salvetti correlation-energy formula into a functional of the electron density. *Phys Rev B Condens Matter.* 1988;37:785-9.
30. Saha SK, Hens A, Roychowdhury A, Lohar AK, Murmu NC, Banerjee P. Molecular dynamics and density functional theory study on corrosion inhibitory action of three substituted pyrazine derivatives on steel surface. *Can Chem Trans.* 2014;2:489-503.
31. Parr RG, Pearson RG. Absolute hardness: companion parameter to absolute electronegativity. *J Am Chem Soc.* 1983;105:7512-6.
32. Chermette H. Chemical reactivity indexes in density functional theory. *J Comput Chem.* 1999;20:129-54.
33. Pearson RG. Absolute electronegativity and hardness: application to inorganic chemistry. *Inorg Chem.* 1988;27:734-40.
34. Saha SK, Ghosh P, Hens A, Murmu NC, Banerjee P. Density functional theory and molecular dynamics simulation study on corrosion inhibition performance of mild steel by mercaptoquinoline Schiff base corrosion inhibitor. *Physica E.* 2015;66:332-41.
35. Ashassi-Sarkhadi H, Asghri E. Effect of hydrodynamic conditions on the inhibition performance of L-methionine as a "green" inhibitor. *Electrochim Acta.* 2008;54:162.
36. Zhang QB, Hua YX. Corrosion inhibition of mild steel by alkylimidazolium ionic liquids in hydrochloric acid. *Electrochim Acta.* 2009;54:1881-7.
37. Labjar N, Lebrini M, Bentiss F, Chihib NE, El Hajjaji S, Jama C. Corrosion inhibition of carbon steel and antibacterial properties of aminotris (methylphosphonic) acid. *Mater Chem Phys.* 2010;119:330-6.
38. Galai M, El Gouri M, Dagdag O, El Kacimi Y, Elharfi A, Ebn Touhami M. New hexa propylene glycol cyclotriphosphazene as efficient organic inhibitor of carbon steel corrosion in hydrochloric acid medium. *J Mater Environ Sci.* 2016;7:1562.
39. Ehteshamzadeh M, Jafari AH, Naderi E, Hosseini MG. Two new Schiff base compounds on inhibition performance in 1M HCl solution by EIS. *Mater Chem Phys.* 2009;113:986-93.
40. Galai M, Ouassir J, Ebn Touhami M, Nassali H, Benqilou H, Belhaj T, et al. α -Brass and $(\alpha + \beta)$ brass degradation processes in azrou soil medium used in plumbing devices. *J Bio-Tribo-Corros.* 2017;3:30.
41. Li X, Xie X, Deng S, Du G. Two phenylpyrimidine derivatives as new corrosion inhibitors for cold rolled. *Corros Sci.* 2014;87:27-39.
42. Laabaissi T, Lgaz H, Oudda H, Benhiba F, Zarrok H, Zarrouk A, et al. Comparative study of corrosion inhibition effect of benzodiazepine derivative on the carbon steel surface in 2.0 M H₃PO₄ and 1.0 M HCl mediums: electrochemical, theoretical and Monte Carlo simulations studies. *J Mater Environ Sci.* 2017;8(3):1054-67.
43. El Makrini B, Lgaz H, Larouj M, Salghi R, Hasan AR, Belkhaoua M, et al. The inhibition performance of sulfamerazine for corrosion of mild steel in HCl. *Pharma Chem.* 2016;8(2):256-68.
44. Tang Y, Zhang F, Hu S, Cao Z, Wu Z, Jing W. Novel benzimidazole derivatives as corrosion inhibitors of mild steel in the acidic media. Part I: gravimetric, electrochemical, SEM and XPS studies. *Corros Sci.* 2013;74:271-82.
45. Methal A, Koulou A, El Bakri M, Touhami ME, Galai M, Lakhri M, et al. Green approach to corrosion inhibition of mild steel in 1 M HCl solutions by Monosaccharides derivatives. *Maghreb J Pure & Appl. Sci.* 2015;1(2):46-61.
46. Aal MA, Radwan S, El-Saied A. Phenothiazines as corrosion inhibitors for zinc in NH₄Cl solution. *Br Corros J.* 1983;18(2):102-6.
47. Tsuru T, Haruyama S, Gijutsu B. Corrosion inhibition of iron by amphoteric surfactants in 2M HCl. *J Jpn Soc Corros Eng.* 1978;27:573-81.
48. Peters W, Portus JH, Robinson BL. The chemotherapy of rodent malaria, XXII: the value of drug-resistant strains of *P. berghei* in screening for blood schizontocidal activity. *Ann Trop Med Parasitol.* 1975;69(2):155-71.
49. Choi DJ, You SJ, Kim JG. Development of an environmentally safe corrosion, scale, and microorganism inhibitor for open recirculating cooling systems. *Mater Sci Eng A.* 2002;335(1-2):228-35.
50. Zulfareen N, Kannan K, Venugopal T, Gnanavel S. Synthesis, characterization and corrosion inhibition efficiency of N-(4-(Morpholinomethyl Carbamoyl Phenyl) Furan-2-Carboxamide for brass in HCl medium. *Arab J Chem.* 2016;9(1):121-35.
51. Oguzie EE. Corrosion inhibitive effect and adsorption behaviour of Hibiscus sabdariffa extract on mild steel in acidic media. *Port Electrochem Acta.* 2008;26(3):303-14.
52. Martinez S, Stern I. Thermodynamic characterization of metal dissolution and inhibitor adsorption processes in the low carbon steel/mimosa tannin/sulfuric acid system. *Appl Surf Sci.* 2002;199(1-4):83-9.
53. Hosseini SMA, Salari M, Ghasemi M, Abaszadeh M. Enaminone compounds as corrosion inhibitors for austenitic stainless steel in sulphuric acid solution. *javascript: filterformular (3).* *Z Phys Chem.* 2009;223(7):769-79.
54. Bloom FE, Kupfer DJ. *Psychopharmacology: the fourth generation of progress - American College of Neuropsychopharmacology.* New York: Raven Press; 1995.
55. Larouj M, Belkhaoua M, Lgaz H, Salghi R, Jodeh S, Samhan S, et al. Experimental and theoretical study of new synthesized organic compounds on corrosion behaviour and the inhibition of carbon steel in hydrochloric acid solution. *De R Pharma Chem.* 2016;8:114-33.
56. Adardour L, Lgaz H, Salghi R, Larouj M, Jodeh S, Zougagh M, et al. Corrosion inhibition of steel in phosphoric acid by sulfapyridine experimental and theoretical studies. *Der Pharmacia Lettre.* 2016;8(4):173-85.
57. Migahed MA, Farag AA, Elsaed SM, Kamal R, Mostfa M, Abd El-Bary H. Synthesis of a new family of Schiff base nonionic surfactants and evaluation of their corrosion inhibition effect on X-65 type tubing steel in deep oil wells formation water. *Mater Chem Phys.* 2011;125(1-2):125-35.
58. Singh A, Lin Y, Quraishi MA, Olasunkanmi LO, Fayemi OE, Sasikumar Y, et al. Porphyrins as corrosion inhibitors for N80 Steel in 3.5% NaCl solution: electrochemical, quantum chemical, QSAR and Monte Carlo simulations studies. *Molecules.* 2015;20(8):15122-46.
59. Noor EA, Al-Moubaraki AH. Thermodynamic study of metal corrosion and inhibitor adsorption processes in mild steel/1-methyl-4 [4'-(X)-styryl] pyridinium iodides/hydrochloric acid systems. *Mater Chem Phys.* 2008;110(1):145-54.
60. Tanak H, Ađar A, Yavuz M. Experimental and quantum chemical calculational studies on 2-[(4-Fluorophenylimino) methyl]-3, 5-dimethoxyphenol. *J Mol Model.* 2010;16(3):577-87.
61. Umoren SA, Eduok UM, Solomon MM, Udoh AP. Corrosion inhibition by leaves and stem extracts of *Sida acuta* for mild steel in 1 M H₂SO₄ solutions investigated by chemical and spectroscopic techniques. *Arab J Chem.* 2016;9:S209-24.
62. Yadav DK, Quraishi MA. Application of some condensed uracils as corrosion inhibitors for mild steel: gravimetric, electrochemical, surface morphological, UV-visible, and theoretical investigations. *Ind Eng Chem Res.* 2012;51(46):14966-79.
63. Abboud Y, Abourriche A, Saffaj T, Berrada M, Charrouf M, Bennamara A, et al. 2, 3-Quinoxalinedioneas a novel corrosion inhibitor for mild steel in 1M HCl. *Mater Chem Phys.* 2007;105:1.
64. Obot IB, Obi-Egbedi NO, Eseola AO. Anticorrosion Potential of 2-Mesityl-1H-imidazo[4,5-f][1,10]-phenanthroline on Mild Steel in Sulfuric Acid Solution: experimental and Theoretical Study. *Ind Eng Chem Res.* 2011;50:2098.

65. Ostovari A, Hoseinieh SM, Peikari M, Shadizadeh SR, Hashemi SJ. Corrosion inhibition of mild steel in 1 M HCl solution by henna extract: A comparative study of the inhibition by henna and its constituents (Lawsonic acid, Gallic acid, α -D-Glucose and Tannic acid). *Corros Sci.* 2009;51(9):1935-49.
66. Tazouti A, Errahmany N, Rbaa M, Galai M, Rouifi Z, Tourir R, et al. Effect of hydrocarbon chain length for acid corrosion inhibition of mild steel by three 8-(n-bromo-R-alkoxy)quinoline derivatives: experimental and theoretical investigations. *J Mol Struct.* 2021;1244:130976.
67. Özcan M, Solmaz R, Kardaş G, Dehri İ. Adsorption properties of barbiturates as green corrosion inhibitors on mild steel in phosphoric acid. *Colloids Surf A Physicochem Eng Asp.* 2008;325(1-2):57-63.
68. Solmaz R. Investigation of the inhibition effect of 5-(E)-4-phenylbuta-1,3-dienylideneamino)-1,3,4-thiadiazole-2-thiol Schiff base on mild steel corrosion in hydrochloric acid. *Corros Sci.* 2010;52(10):3321-30.
69. Fang J, Li J. Quantum chemistry study on the relationship between molecular structure and corrosion inhibition efficiency of amides. *J Mol Struct Theochem.* 2002;593(1-3):179-85.
70. Udhayakala P, Rajendiran TV, Gunasekaran S. Theoretical evaluation of corrosion inhibition performance of some triazole derivatives. *J Adv Sci Res.* 2012;3(2):71-7.
71. Amin MA, Khaled KF, Mohsen Q, Arida HA. A study of the inhibition of iron corrosion in HCl solutions by some amino acids. *Corros Sci.* 2010;52(5):1684-95.
72. Murulana LC, Singh AK, Shukla SK, Kabanda MM, Ebenso EE. Experimental and quantum chemical studies of some bis (trifluoromethyl-sulfonyl) imide imidazolium-based ionic liquids as corrosion inhibitors for mild steel in hydrochloric acid solution. *Ind Eng Chem Res.* 2012;51(40):13282-99.
73. Abdel-Ghani NT, El-Ghar MFA, Mansour AM. Novel Ni (II) and Zn (II) complexes coordinated by 2-arylaminoethyl-1H-benzimidazole: molecular structures, spectral, DFT studies and evaluation of biological activity. *Spectrochim Acta A Mol Biomol Spectrosc.* 2013;104:134-42.
74. Peme T, Olasunkanmi LO, Bahadur I, Adekunle AS, Kabanda MM, Ebenso EE. Adsorption and corrosion inhibition studies of some selected dyes as corrosion inhibitors for mild steel in acidic medium: gravimetric, electrochemical, quantum chemical studies and synergistic effect with iodide ions. *Molecules.* 2015;20(9):16004-29.
75. Nwankwo HU, Olasunkanmi LO, Ebenso EE. Experimental, quantum chemical and molecular dynamic simulations studies on the corrosion inhibition of mild steel by some carbazole derivatives. *Sci Rep.* 2017;7(1):2436.
76. Udhayakala P, Rajendiran TV. A theoretical evaluation on benzothiazole derivatives as corrosion inhibitors on mild steel. *Der Pharma Chem.* 2015;7(1):92-9.
77. El Faydy M, Tourir R, Touhami ME, Zarrouk A, Jama C, Lakhri B, et al. Corrosion inhibition performance of newly synthesized 5-alkoxymethyl-8-hydroxyquinoline derivatives for carbon steel in 1 M HCl solution: experimental, DFT and Monte Carlo simulation studies. *Phys Chem Chem Phys.* 2018;20(30):20167-87.
78. Olasunkanmi LO, Obot IB, Kabanda MM, Ebenso EE. Some quinoxalin-6-yl derivatives as corrosion inhibitors for mild steel in hydrochloric acid: experimental and theoretical studies. *J Phys Chem C.* 2015;119(28):16004-19.